

# Finite Element Modeling of Microstructural Changes During Equal Channel Angular Drawing of Pure Aluminium

SERAFINO CARUSO (✉ [serafino.caruso@unical.it](mailto:serafino.caruso@unical.it))

University of Calabria: Universita della Calabria <https://orcid.org/0000-0003-4090-6133>

Stano Imbrogno

University of Birmingham

---

## Research Article

**Keywords:** Microstructural changes, Dynamic recrystallisation, Grain size, Aluminium, Finite element modeling, Equal channel angular drawing

**Posted Date:** March 9th, 2021

**DOI:** <https://doi.org/10.21203/rs.3.rs-191945/v1>

**License:**   This work is licensed under a Creative Commons Attribution 4.0 International License.

[Read Full License](#)

---

**Version of Record:** A version of this preprint was published at The International Journal of Advanced Manufacturing Technology on March 29th, 2021. See the published version at <https://doi.org/10.1007/s00170-021-06972-0>.

# FINITE ELEMENT MODELING OF MICROSTRUCTURAL CHANGES DURING EQUAL CHANNEL ANGULAR DRAWING OF PURE ALUMINIUM

Serafino Caruso<sup>1\*</sup>, Stano Imbrogno<sup>2</sup>

<sup>1</sup> Department of Mechanical, Energy and Management Engineering, University of Calabria, Rende, CS 87036, Italy. ORCID: 0000-0003-4090-6133

<sup>2</sup> School of Metallurgy and Materials, University of Birmingham, Birmingham B15 2TT, UK. ORCID: 0000-0002-9988-9860

Corresponding author.

E-mail address: serafino.caruso@unical.it (S. Caruso)

## ABSTRACT

*Grain refinement by severe plastic deformation (SPD) techniques, as a mechanism to control microstructure (recrystallization, grain size changes,...) and mechanical properties (yield strength, ultimate tensile strength, strain, hardness variation...) of pure aluminium conductor wires, is a topic of great interest for both academic and industrial research activities. This paper presents an innovative finite element (FE) model able to describe the microstructural evolution and the continuous dynamic recrystallization (CDRX) that occur during equal channel angular drawing (ECAD) of commercial 1370 pure aluminium (99.7% Al). A user subroutine has been developed based on the continuum mechanical model and the Hall-Petch (H-P) equations to predict grain size variation and hardness change. The model is validated by comparison with the experimental results and a predictive analysis is conducted varying the channel die angles. The study provides an accurate prediction of both the thermo-mechanical and the microstructural phenomena that occur during the process characterised by large plastic deformation.*

Keywords: Microstructural changes, Dynamic recrystallisation, Grain size, Aluminium, Finite element modeling, Equal channel angular drawing.

## NOMENCLATURE

A	yield stress
B	numerical constant
C	numerical constant
$C_0$	numerical constant
$C_1$	numerical constant
$C_X$	numerical constant
CPAW	commercially pure aluminium wire
ECAD	equal channel angular drawing
CDRX	continuous dynamic recrystallization
DRX	dynamic recrystallization
FE	finite element
H-P	Hall-Petch
HV	Vickers hardness
SPD	severe plastic deformation
T	current temperature
$T_0$	reference temperature
$T_m$	melting temperature
$\dot{\epsilon}$	strain rate
$\dot{\epsilon}_0$	reference strain rate
$\epsilon$	effective strain
$\epsilon^{p_{eff}}$	effective plastic strain for grain size changes
$\epsilon^p_c$	critical plastic strain for grain size changes
$\Phi$	inner die channel angle
$\Psi$	outer die channel angle
d	average grain size
$d_0$	initial grain size
$d_f$	saturation grain size
$k_y$	numerical constant
$k_X$	numerical constant
$\sigma_y$	yield strength
$\sigma_0$	numerical constant
m	numerical constant
n	numerical constant

## INTRODUCTION

Commercially pure aluminium wire has attracted the interest of automotive industry due to the light weight (a third of steel), corrosion resistance (it naturally generates a protective thin oxide coating), good electrical conductivity, ductility (products near to net shape) and higher mechanical strength to weight ratio. Indeed, aluminium and its alloys are used in vehicles to reduce the dead-weight, energy and fuel consumption while increasing load capacity [1, 2].

Since functional performance and service safety are two aspects of great rank for automotive industry, an accurate knowledge of the microstructural evolution (i.e. grain refinement) that occurs during wire production is required. Indeed, the microstructure is strictly related to the strengthening mechanisms of the material.

In this context, the grain size and recrystallisation are fundamental aspects that need to be controlled for an efficient production development [3-5]. Severe plastic deformation (SPD) processes, in which a high shear strain is imposed on the material, are recognized as the main techniques to achieve microstructural changes by the recrystallisation [6-8].

Many SPD methods were developed during the past three decades [9], but the concept of Equal Channel Angular Drawing (ECAD) [10] represents the most successful SPD technique for continuous production of ultra-fine-grained materials with homogeneous equiaxial microstructure.

In ECAD process the specimen is drawn through a die consisting of two channels of equal cross section intersecting at an angle ( $2\phi$ ), usually between  $90^\circ$  and  $135^\circ$ , preserving its transversal dimension, Fig. 1.

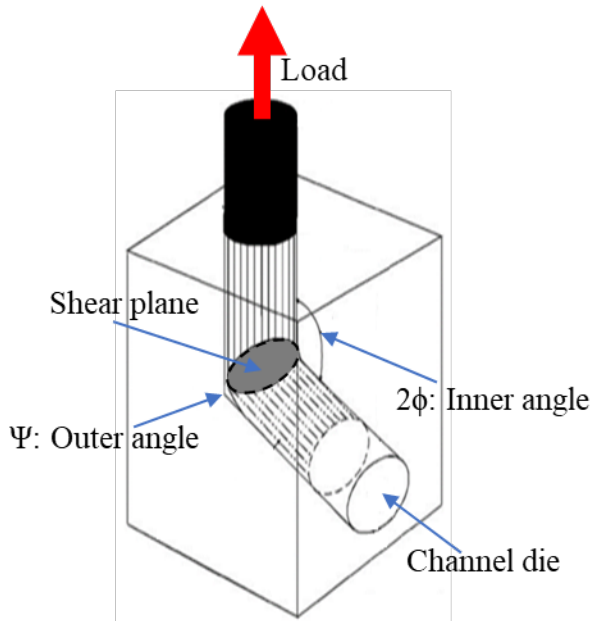


**Fig. 1** Schematic illustration of the ECAD process

Previous works have already investigated and analysed microstructural evolution, SPD and ECAD process of pure aluminium samples.

C. J. Louis Perez et al. [11] investigated the effect of two different processing ways and heat treatments during ECAD process of 1370 aluminium alloy with five passes at room temperature. In particular, the authors processed the workpiece through two different routes: route A (no rotation of the workpiece between the steps) and route B (a 90° rotation of the workpiece at each step). Moreover, two different die channels were implemented for each route. The experimental results confirmed that, compared to the initial condition, a grain refinement occurred leading to recommend the ECAD method as an intermediate process during aluminium alloys wire drawing.

U. Chakkingal et al. [12] investigated the mechanical properties and microstructural evolution of pure aluminium 3004 when processed by 6 passes of ECAD method consisted of two square channels of cross-sectional area 15 x 15 mm<sup>2</sup> intersecting at an angle of 135°. The experimental results showed an increase of the tensile strength, the yield strength,

hardness, and a grain refinement from 2000µm to 1µm.

J. P. Hou et al. [13] analysed the commercially pure aluminium wires (CPAWs) by tensile tests, electron backscatter diffraction (EBSD) and transmission electron microscopy (TEM) observations to establish the relation between the mechanical properties and the microstructural evolution. The outcomes showed as the texture, grain size and dislocation density mainly influence the performance of the material after the drawing process.

A. A. Zisman et al. [14] investigated the mechanical properties, the textures and microstructures of the sheet metals processed by a new simple method of ECAD, with adjustable die opening, comparing the obtained results with closely related process technique.

Y. K. Zhu et al. [15] examined the effect of the stress profile on the texture evolution of the CPAW by combining the numerical results with the microstructural observations. A FE model was developed to better understand the relationship between the stress profile and the microstructural evolution during the multi-pass cold drawing of the CPAW. The results showed the plastic deformation mode on the wire cross section, the stress contribution to the texture formation and the average grain size evolution from the wire surface to its centre.

U. Chakkingal et al. [16] presented a study of three different routes of the ECAD process on pure commercial aluminium bars with extremely coarse grains (of the order of 2000µm in size). The outcomes showed a significant increase in tensile and yield strengths, with a corresponding decrease in ductility. Moreover, micro-sized sub-grains with a shape varying from elongated to equiaxed were obtained. The authors highlighted the usefulness of ECAD process as a continuous industrial method to produce grain-refined bars with increased strength from coarse-grained aluminium.

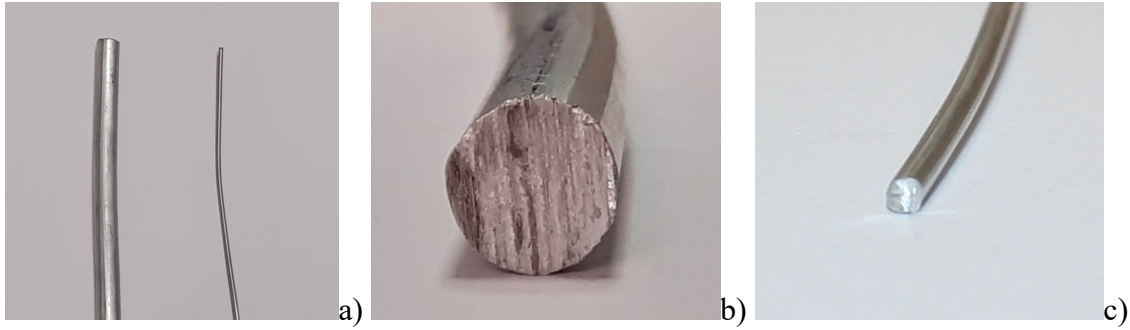


**Fig. 2** a) Analysed samples, b) Initial aluminium rod  $\phi=9.50\text{mm}$ , c) Cold-drawn wire  $\phi=2.00\text{mm}$

All these studies suggest the important role of the microstructural evolution in enhancing the mechanical properties of the aluminium alloys as well as the suitability of the ECAD processes for refining the grain structure. Therefore, it is also useful to develop an adequate FE numerical model to predict and control the thermo-mechanical phenomena that occur during the investigated processes since they are fundamental for the mechanical performances and the quality of the final product.

In this paper an advanced flow stress empirical model that includes the grain size variation was developed to predict the material behaviour of commercial 1370 pure aluminium wires (Al 99.7%) during ECAD process. Once defined all the constants of the material flow stress model, a continuum mechanical model and H-P equation were implemented by two customized user sub-routines. Therefore, the developed model was able to predict the grain refinement and hardness variation during the investigated process. Finally, a comparison between numerical results and the corresponding experimental data was carried out to validate the developed model and to show the effectiveness of the proposed numerical tool.

## EXPERIMENTAL PROCEDURE

Commercial 1370 pure aluminium rods (Table 1) with an initial diameter of 9.50mm were analysed. A multiple-pass cold drawing was performed at room

temperature to produce wires with final diameter of 2.00mm after 15 passes, with a total section reduction of 95.6% and a total drawing strain of 3.11 (Fig. 2).

**Table 1** Material chemical composition

Al	Si	Fe	Cu	Mn	Mg
99.7	0.10	0.25	0.02	0.01	0.02
Cr	Ni	Zn	B	Ga	
0.01	-	0.04	0.02	0.03	

ECAD process, with an inner die angle  $\Phi=140^\circ$  and outer die angle  $\psi=\pi-\Phi$ , as shown in Fig. 3, was performed at room temperature on the cold-drawn wires preserving their transversal dimensions, with a drawing speed of 25m/sec.

Uniaxial tensile tests of the aluminium rods, drawn wires and ECAD processed wires were carried out using the MTS Criterion Model 45 testing machine and all the tests were performed at room temperature. In particular, nine samples (three aluminium rods, three drawn-wires and three ECAD processed wires) were analysed and the average value of the stress-strain profile measured for the three type of samples, is reported in Fig. 4.

The tensile tests show as the material strength was enhanced when both drawing and ECAD process are performed on the aluminium wire. In detail, the value of the yield strength and the ultimate tensile strength were higher while the ductility decreased, indeed the

true strain ( $\epsilon$ ) dropped from 0.11 to 0.08 after cold-drawing. This result agrees with X. M. Luo

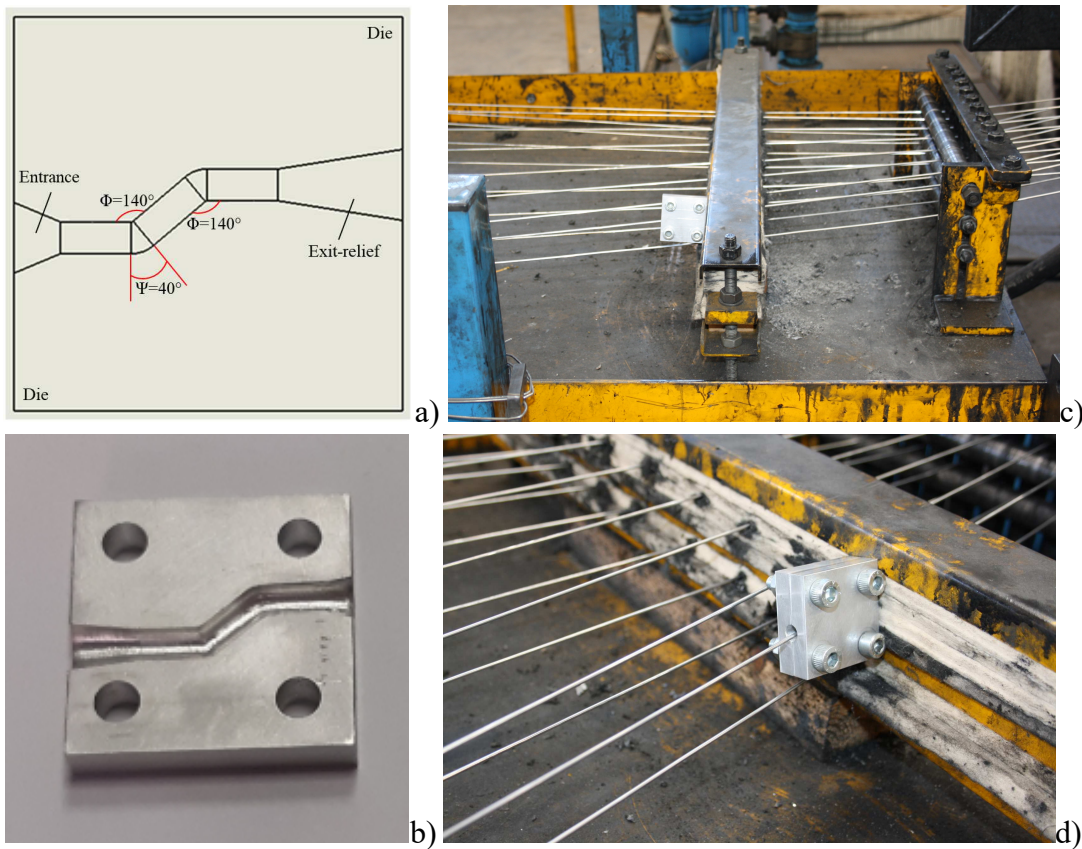


**Fig. 3** a-b) Geometry of the ECAD die, c-d) Experimental set-up

et al. [17] outcomes. Indeed, they demonstrated an increase of the yield strength and a decrease of the elongation when drawing pure aluminium wire from an initial diameter of 9.5mm to 2.99mm after 9 passes. Moreover, a further enhancement of 30MPa in material strength was observed after ECAD process on drawn wires with a reduction of the true strain of 0.04. The plastic deformation of each drawing pass and the SPD imposed by ECAD die led to an increase of the material strength due to the hardening effect produced by the accumulation of the dislocations [13, 18] and the Hall-Petch (H-P) effect induced by the microstructural phenomena (i.e. grain refinement).

Subsequently, samples of initial aluminium rods, cold-drawn wires and ECAD processed wires were cut and the transverse section was mounted into a resin holder for the microstructural analysis.

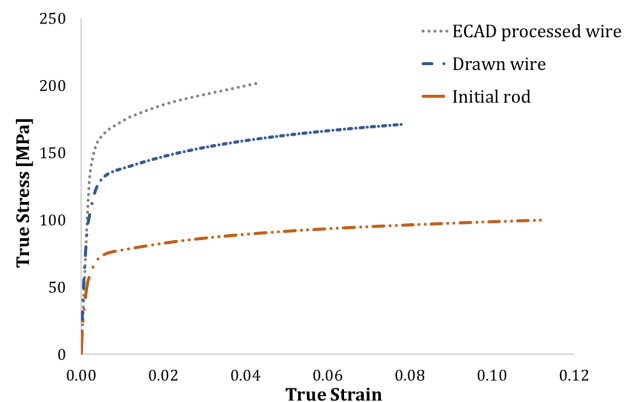


**Fig. 4** True stress-strain curve

The metallographic preparation consisted of mechanical polishing and then etching by the use of Keller's reagent (92ml of distilled water, 6ml of nitric acid, 2ml of hydrochloric acid, 2ml hydrofluoric acid). The cross section of the three samples was analysed using an optical microscope for microstructural analysis, while the micro-hardness ( $HV_{0.01}$ ) was investigated by an instrumented micro-nano indenter.

In Fig. 5 are reported the micrographs obtained by the optical microscopy analysis. In Fig. 5a the grains are analysed under polarised light to better show the grain morphology. It is possible to observe that the grains, although the elliptical shape, mostly look equiaxial and the average measured diameter was equal to  $58\mu\text{m}$ . In Fig. 5b and 5c are reported the

grains structure after the cold-drawn and the ECAD respectively. It is clear the effect of the drawing process on the grain refinement. In Fig. 5b the grains still maintain their morphology (grain boundaries represented by the black and thicker lines) although the size is significantly reduced and the average value was equal to  $11\mu\text{m}$ . Finally, in Fig. 5c the micrograph shows the cross section of the ECAD sample. It appears also in this case the grain refinement induced by the ECAD and a change in the grain morphology (grains shape more equiaxial than elliptical). For this latter sample the average measured grain size was equal to  $6\mu\text{m}$ . Considering the initial grain size of the aluminium rods ( $58\mu\text{m}$ ), the total processes deformations allowed to reach an overall reduction of 81%, Fig. 5.

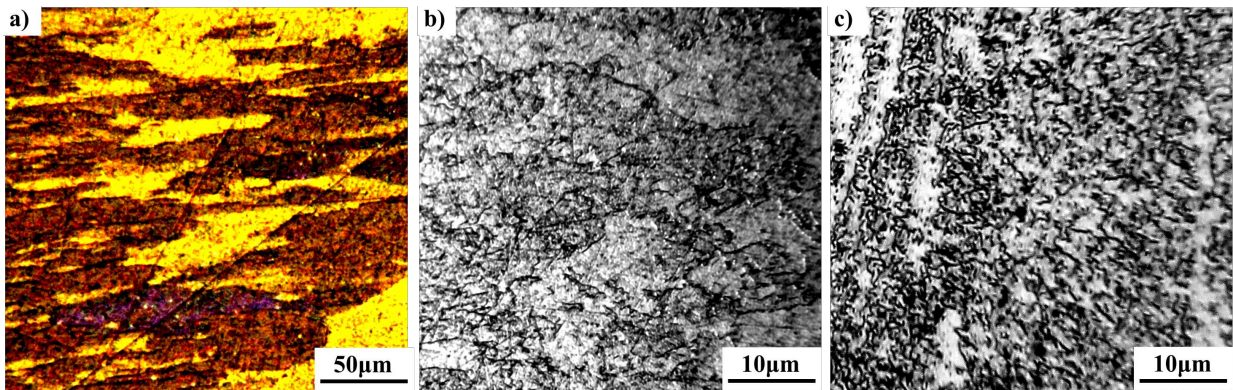


**Fig. 5** Transverse section microstructure a) initial aluminium rod (polarised light), b) cold-drawn wire (bright field) and c) ECAD processed wire (bright field)

The micro-hardness was measured on nine samples (three aluminium rods, three drawn-wires and three ECAD processed wires), and ten indentations per sample were carried out for a total of 90 tests and the average value was considered (Fig. 6). A significant increase of 14HV was first observed at the end of the 15 drawing passes and 9HV more after

ECAD process for a total hardness increase of 59%. In both cases, the hardness variation is mainly due to the evolution of the microstructure, during the large strain, that results in grain refinement due to the dynamic recrystallization (DRX) phenomena as well as work hardening.

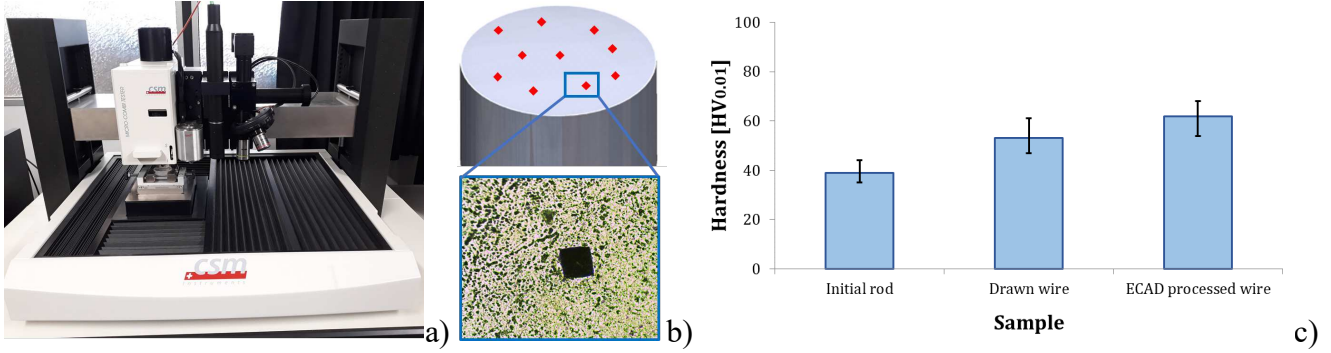


**Fig. 6** Transverse section hardness a) micro-nano indenter, b) transverse section indentation analysis and c) measurements

## NUMERICAL MODEL

The commercial FE software SFTC DEFORM-3D<sup>TM</sup> has been used to simulate the ECAD process of commercial 1370 pure aluminium drawn-wire using coupled thermo-mechanical analysis with automatic remeshing. The workpiece was modelled as a plastic body meshed with 50000 isoparametric tetrahedral elements, while for the die a rigid model with 64000 elements was considered (Fig. 7).

To simulate the material behaviour under SPD condition a modified Johnson-Cook (J-C) flow stress model was developed. According to the original J-C model the flow stress is expressed as (Equation 1).

$$\sigma(\varepsilon, \dot{\varepsilon}, T) = (A + B\varepsilon^n) \left( 1 + C \ln \left( \frac{\dot{\varepsilon}}{\dot{\varepsilon}_0} \right) \right) \left( 1 - \left( \frac{T - T_0}{T_m - T_0} \right)^m \right) \quad (1)$$

Where  $A$  is the yield stress at reference temperature and strain rate,  $B$  and  $n$  respectively the coefficient and the exponent of strain hardening,  $C$  the coefficient of strain rate hardening,  $\varepsilon$  is the equivalent plastic strain,  $\dot{\varepsilon}$  and  $\dot{\varepsilon}_0$  are the plastic strain rate and the reference plastic strain rate respectively.  $T_0$  is the reference temperature,  $T_m$  is the melting temperature and  $m$  the thermal softening exponent.

The model proposed in this research modified the constant  $A$  (MPa) of the flow stress in Equation 1 to consider the influence of the grain refinement caused by DRX according to H-P equation (Equation 2).

$$A = \sigma_y = \sigma_0 + \frac{k_y}{\sqrt{d}} \quad (2)$$

Where  $\sigma_y$  is the yield strength,  $k_y$  is the strengthening coefficient,  $\sigma_0$  is a material constant and  $d$  is the average grain size.

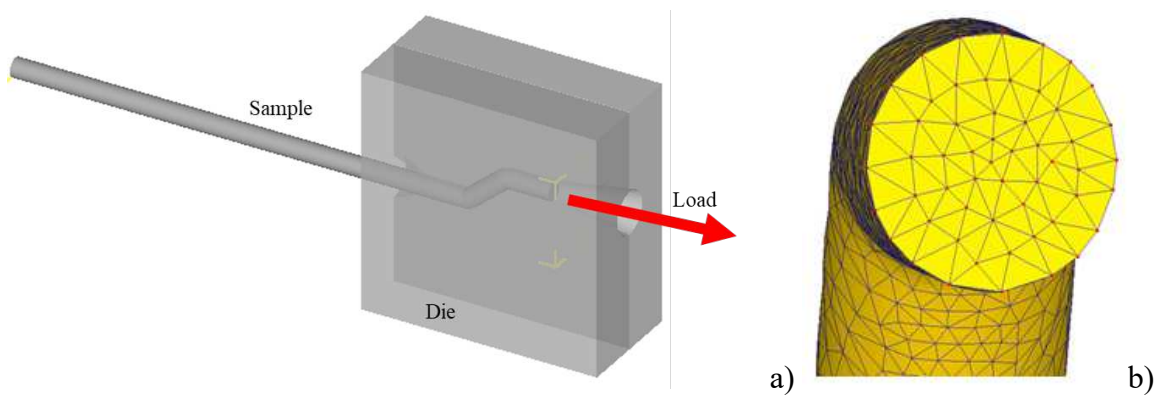


**Fig. 7** a) FE model and b) wires discretization

By this modification, the material flow stress is influenced by the DRX that significantly modifies the microstructure of the material resulting in the material strengthening described by the Hall-Petch (H-P) effect.

Thus, the thermo-mechanical behaviour of the pure aluminium is numerically represented by the new modified J-C law (Equation 3).

$$\sigma(\varepsilon, \dot{\varepsilon}, T, d) = \left( \left( \sigma_0 + \frac{k_y}{\sqrt{d}} \right) + B\varepsilon^n \right) \left( 1 + C \ln \left( \frac{\dot{\varepsilon}}{\dot{\varepsilon}_0} \right) \right) \left( 1 - \left( \frac{T - T_0}{T_m - T_0} \right)^m \right) \quad (3)$$

A regression approach was implemented to determine the values of the numerical constants  $B$ ,  $n$ ,  $C$ , and  $m$ , performing uniaxial tensile tests of the aluminium rods with three different speeds and temperatures (Table 2). Moreover, for each tensile test condition three tests were considered in order to assess the statistical reliability for a total of 27 experiments and finally the average value was measured.

**Table 2** Tensile test conditions

Test speed (mm/sec)			Temperature (°C)		
0.1	10	20	20	80	140

The numerical constants  $\sigma_0$  and  $k_y$  were determined by Equation 2 through the previously measured values of the yield strength and the grain size of both initial aluminium rods and drawn wires.

All the coefficients of the material behaviour model are listed in Table 3.

**Table 3** Numerical material model parameters

<b>B</b>	<b>n</b>	<b>C</b>	<b>m</b>	<b><math>\sigma_0</math></b>	<b><math>k_y</math></b>
104.2	0.385	0.0097	1.175	16.39	370.14

The physical events that affect the mechanical properties were predicted by implementing a customized user subroutine with a CDRX model for the grain refinement [18-20] and the H-P equation to predict the hardness evolution.

In particular, the CDRX represents the main physics metallurgical phenomenon due to the nature of the material used (pure aluminium) [21-23], therefore a continuum mechanical model to predict the grain size was implemented, Equation 4.

$$d = d_0 - (d_0 - d_f)(1 - \exp(-k_x < \varepsilon^p_{eff} - \varepsilon^p_c >^{c_x})) \quad d_f \leq d \leq d_0 \quad (4)$$

Where  $d$  is the recrystallized grain size,  $d_0$  the initial grain size,  $d_f$  the saturation grain size,  $k_x$  and  $c_x$  are parameters describing the recrystallization evolution with increasing plastic deformation. The McCauley brackets  $< >$  indicate that recrystallization phenomena will occur when the effective strain  $\varepsilon^p_{eff}$  will reach the threshold value  $\varepsilon^p_c$ . The model developed by Y. Iwahashi et al. [24] was considered for the ECAD process strain  $\varepsilon^p_{eff}$  (Equation 5).

$$\varepsilon^p_{eff} = \left( \frac{N_{pass}}{3^{0.5}} \right) \left( 2 \cot \left( \frac{\Phi}{2} + \frac{\Psi}{2} \right) + \psi \operatorname{cosec} \left( \frac{\Phi}{2} + \frac{\Psi}{2} \right) \right) \quad (5)$$

Where  $\Phi$  and  $\psi$  are the ECAD die angles (Fig. 3) and  $N_{pass}$  is the number of ECAD passes.

While the parameters  $k_x$  and  $c_x$  and the critical strain leading to CDRX were set 3.8, 2 and 0.1 according to [21] respectively.

Finally, the hardness modification depending on the recrystallized grain size was calculated according to the H-P equation that considers hardness evolution as an inverse function of grain size (Equation 6):

$$HV = C_0 + \frac{C_1}{\sqrt{d}} \quad (6)$$

Where  $C_0$  and  $C_1$  are two material constants while  $d$  represents the average grain size. The value of  $C_0$  and  $C_1$ , were determined through the previously measured values of the material hardness and grain size of both initial aluminium rods and drawn wires and were equal to 28.2 and 82.2, respectively.

### FE VALIDATION AND RESULTS

The FE model was validated by comparing the experimental results of hardness variation and the grain size evolution with the corresponding numerical data.

Fig. 8 reports the stable and uniform data prediction of grain refinement and hardness variation and it is possible to observe the effectiveness of the customized model and the user subroutines to successfully predict the phenomena that occur during the ECAD process. In particular, the CDRX takes place since the SPD induced by the die geometry allows the effective strain  $\varepsilon^{p_{eff}}$  to overcome the threshold value  $\varepsilon^p_c$ . Therefore, a new grain size is calculated and the microstructural changes affect the material behaviour according to Equation 3.

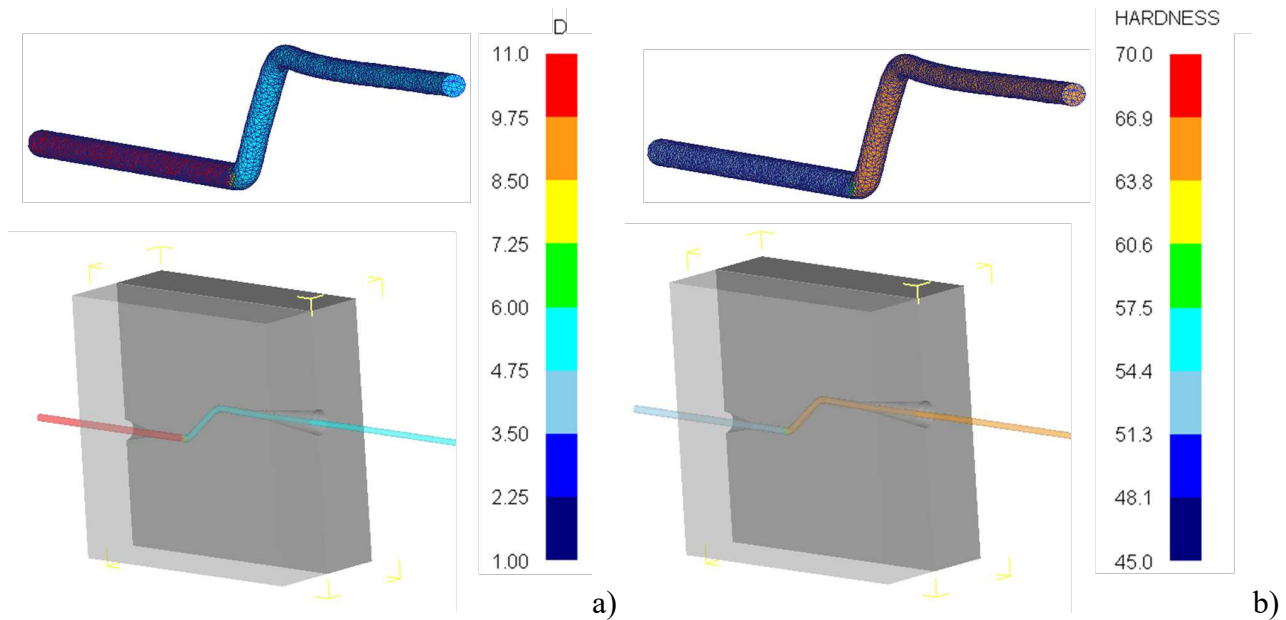


**Fig. 8** Numerical prediction of a) grain size ( $\mu\text{m}$ ) and b) hardness ( $\text{HV}_{0.01}$ ).

The predicted grain size evolution and the hardness variation were measured along five different cross sections of the ECAD processed wire.

According to the experimental outcomes the numerical results show that after the ECAD die, the internal evolution of the microstructural features results in an average grain size that decreases becoming the half size of the as cold-drawn. Thus, according to the inverse function of H-P equation (Equation 6), the hardness increases confirming that

the ECAD process causes severe microstructural and mechanical properties changes (Fig. 9).

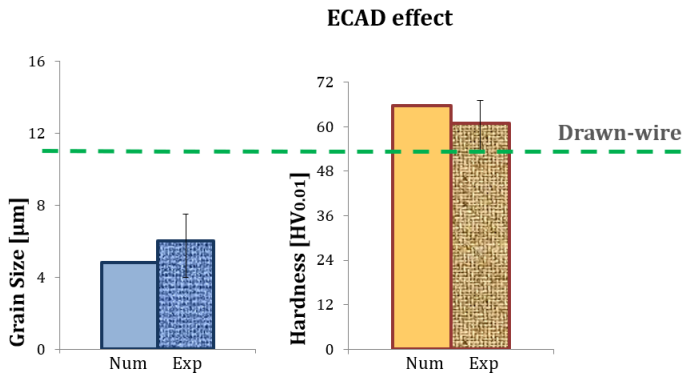


**Fig. 9** Comparison between measured and predicted grain size and hardness variation

Fig. 9 shows the comparison between the numerical results and the corresponding experimental data. The comparison analysis highlighted a small difference of  $1.2\mu\text{m}$  regarding grain size evolution and a relative error of 8% when the hardness changes

is predicted. This slight differences between the numerical and the experimental data suggest that the developed numerical procedure is enough robust. The reason of the small difference between numerical and experimental results could be related to both the accuracy of the experimental data and the calibration procedure used to define all the numerical constants of the equations implemented in the user subroutine.

After the validation of the numerical model, a predictive analysis was carried out with the aim to analyse the evolution of the grain size and hardness change when the  $\Phi$  die angle is modified. In particular, different simulations were carried out increasing the inner die angle  $\Phi$  to  $165^\circ$  and  $175^\circ$  with a corresponding outer die angle  $\psi = \pi - \Phi$  (Fig. 10 and Fig. 11). The numerical results are listed in Table 4.

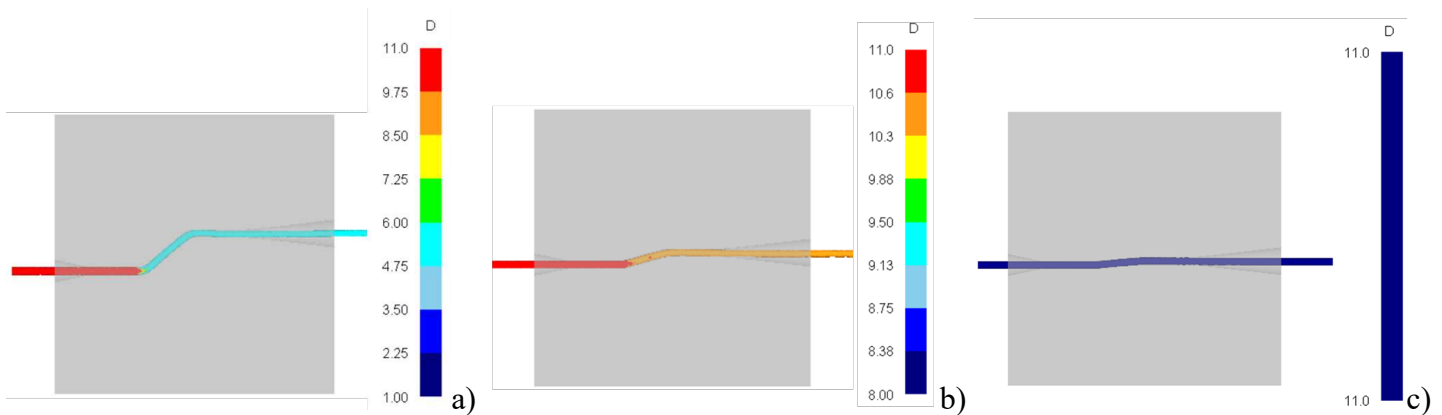


**Fig. 10** Grain size predictive numerical analysis: a)  $\Phi=140^\circ$ , b)  $\Phi=165^\circ$ , c)  $\Phi=175^\circ$

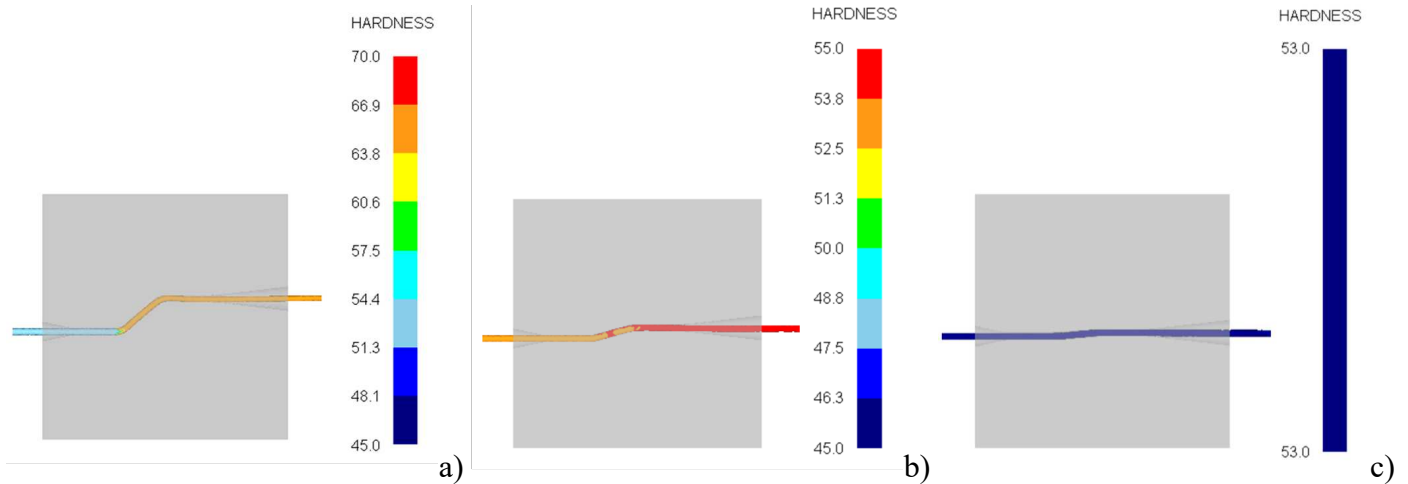


**Fig. 11** Hardness predictive numerical analysis: a)  $\Phi=140^\circ$ , b)  $\Phi=165^\circ$ , c)  $\Phi=175^\circ$

**Table 4** Predictive analysis results

$\Phi$ [°]	$d_0$ [ $\mu\text{m}$ ]	$d_f$ [ $\mu\text{m}$ ]	Reduction [%]	$HV_{\text{initial}}$	$HV_{\text{final}}$	Rise [%]
140	11	4.8	56	53	65.7	24
165	11	10.3	6	53	53.8	2
175	11	11.0	0	53	53	0

The predictive analysis highlights as the effectiveness of the investigated ECAD process is related to a limited range of  $\Phi$  die angle, between  $140^\circ$  and  $165^\circ$  because the channel geometry leads a heavy deviation that results in SPD. Thus, the plastic deformation affects the microstructure of the aluminium triggering the grain refinement process. While high values of the  $\Phi$  die angle results in low plastic strain hence the strengthening effect due to the grain size evolution decreases. Considering the application of the ECAD as a continuous industrial processing step, these results are significantly important since they suggest the impact of the microstructural changes effects and the mechanical properties of the final product as a function of the process parameters and channel die geometry.

## DISCUSSION AND CONCLUSIONS

In this research article an advanced empirical model, including grain size evolution, was developed to describe the material behaviour of commercial 1370 pure aluminium wires (Al 99.7%) during ECAD process.

A continuum mechanical model and the H-P effect were implemented for predicting the grain size and the hardness evolutions. A new modified J-C model was implemented considering the effect of grain size on the material behaviour during the SPD process. By this modification, the material flow stress is influenced by the CDRX that significantly modifies the microstructure of the material (i.e. grain refinement) resulting in material strengthening for the H-P effect.

The numerical results were validated by comparison with those experimentally found demonstrating the effectiveness of the customized model and the user subroutines to successfully predict the CDRX phenomenon, taking place during the ECAD process, due to the high strains induced by SPD.

Finally, a predictive numerical analysis showed the main importance of the die channel geometry in controlling the microstructural changes of the material as well as the mechanical behaviour and the hardening effect.

Thus, the proposed FE strategy can be used to properly simulate the material behaviour of commercial 1370 pure aluminium wires (Al 99.7%) during ECAD process. The model allows to take into account the microstructural characteristics of the material that affect the material flow stress and the hardness. The developed numerical tool can be potentially employed during the design step of the drawing process to accurately achieve the desired mechanical performances required by the product.

## DECLARATIONS

**Funding:** Not applicable.

**Conflicts of interest/Competing interests:** The authors have no conflicts of interest to declare that are relevant to the content of this article.

**Availability of data and material:** Not applicable

**Code availability:** commercial FE software SFTC DEFORM-3D™

**Authors' contributions:** Conceptualization, S.C. and S.I.; methodology, S.C. and S.I. software, S.C.; validation, S.C.; formal analysis, S.I.; investigation, S.C. and S.I.; resources, S.C. and S.I.; data curation, S.C. and S.I.; writing—original draft preparation, S.C. and S.I.; writing—review and editing, S.C. and S.I.; visualization, S.I.; supervision, S.C. All authors have read and agreed to the published version of the manuscript.

**Ethics approval:** Not applicable.

**Consent to participate:** Not applicable

**Consent for publication:** Not applicable

## REFERENCES

- [1] Krishna G V, De T N, Burman R K, Sekhar B V, Rao V G (2019) Numerical and experimental comparative study of Aluminum and hybrid mounting interfaces of launch vehicle avionics for weight reduction. *Procedia Struct Integrity* 14: 820-829. <https://doi.org/10.1016/j.prostr.2019.07.060>.
- [2] Palazzo J, Geyer R (2019) Consequential life cycle assessment of automotive material substitution: Replacing steel with aluminum in production of north American vehicles. *Environ Impact Assess Rev* 75: 47-58. <https://doi.org/10.1016/j.eiar.2018.12.001>.
- [3] Sakai T, Jonas J J (1984) Overview n.35 Dynamic recrystallization: mechanical and microstructural considerations. *Acta Metal* 32(2): 189-209. [https://doi.org/10.1016/0001-6160\(84\)90049-X](https://doi.org/10.1016/0001-6160(84)90049-X).
- [4] Busso E P (1998) A continuum theory for dynamic recrystallization with microstructure-related length scales. *Int J Plast* 14(4-5): 319-353. [https://doi.org/10.1016/S0749-6419\(98\)00008-4](https://doi.org/10.1016/S0749-6419(98)00008-4).
- [5] Zhao H, Ren Y, Yang B, Qin G (2019) Microstructural evolution of equal channel angular drawn purity titanium at room temperature. *J Alloys Compd* 811: 152002. <https://doi.org/10.1016/j.jallcom.2019.152002>.
- [6] Pu Z W, Caruso S, Umbrello D, Dillon O W, Puleo D A, Jawahir I S (2011) Analysis of surface integrity in dry and cryogenic machining of AZ31B Mg alloys. *Adv Mat Res* 223:439-448. <https://doi.org/10.4028/www.scientific.net/AMR.223.439>.
- [7] Zhilyaev A P, Swisher D L, Oh-ishi K, Langdon T G, McNelley T R (2006) Microtexture and microstructure evolution during processing of pure aluminum by repetitive ECAP. *Mater Sci*

- Eng A 429(1-2): 137-148.  
<https://doi.org/10.1016/j.msea.2006.05.009>.
- [8] Suwas S, Arruffat Massion R, Tóth L S, Fundenberger J J, Beausir B (2009) Evolution of texture during equal channel angular extrusion of commercially pure aluminum: Experiments and simulations. *Mater Sci Eng A* 520(1-2): 134-146.  
<https://doi.org/10.1016/j.msea.2009.05.028>.
- [9] Faraji G, Torabzadeh H (2019) An overview on the continuous severe plastic deformation methods. *Mater Trans* 60(7): 1316-1330.  
<https://doi.org/10.2320/matertrans.MF201905>.
- [10] Suriadi A B, Thomson P F (1997) Control of deformation history for homogenizing and optimizing mechanical properties of metals. *Proceedings of Australasia-Pacific Forum on Intelligent Processing & Manufacturing of Materials, IPMM*. 920–926.
- [11] Luis Pérez C J, Berlanga C, Pérez-Ilzarbe J (2003) Processing of aluminium alloys by equal channel angular drawing at room temperature. *J Mater Process Technol* 143–144: 105–111.  
[https://doi.org/10.1016/S0924-0136\(03\)00329-7](https://doi.org/10.1016/S0924-0136(03)00329-7).
- [12] Chakkingal U, Suriadi A B, Thomson P F (1998) Microstructure development during equal channel angular drawing of Al at room temperature, *Scr Mater* 39(6): 677-684.  
[https://doi.org/10.1016/S1359-6462\(98\)00234-6](https://doi.org/10.1016/S1359-6462(98)00234-6).
- [13] Hou J P, Wang Q, Yang H J, Wu X M, Li C H, Li X W, Zhang Z F (2015) Microstructure evolution and strengthening mechanisms of cold-drawn commercially pure aluminum wire. *Mater Sci Eng A* 639: 103-106.  
<https://doi.org/10.1016/j.msea.2015.04.102>.
- [14] Zisman A A, Rybin V V, Van Boxel S, Seefeldt M, Verlinden B (2006) Equal channel angular drawing of aluminium sheet. *Mater Sci Eng A* 427(1-2): 123-129.  
<https://doi.org/10.1016/j.msea.2006.04.007>.
- [15] Zhu Y k, Chen Q Y, Wang Q, Yu H Y, Li R, Hou J P, Zhang Z J, Zhang G P, Zhang Z F (2018) Effect of stress profile on microstructure evolution of cold-drawn commercially pure aluminum wire analyzed by finite element simulation. *J Mater Sci Technol* 34(7): 1214-1221,  
<https://doi.org/10.1016/j.jmst.2017.07.011>.
- [16] Chakkingal U, Suriadi A B, Thomson P F (1999) The development of microstructure and the influence of processing route during equal channel angular drawing of pure aluminum, *Mater Sci Eng A* 266(1-2): 241-249.  
[https://doi.org/10.1016/S0921-5093\(98\)01129-0](https://doi.org/10.1016/S0921-5093(98)01129-0).
- [17] Luo X M, Song Z M, Li M L, Wang Q, Zhang G P (2017) Microstructural evolution and service performance of cold-drawn pure aluminum conductor wires. *J Mater Sci Technol* 33(9): 1039–1043.  
<https://doi.org/10.1016/j.jmst.2016.11.018>.
- [18] Hallberg H (2011) Approaches to modeling of recrystallization. *Metals* 1(1): 16-48.  
<https://doi.org/10.3390/met1010016>.
- [19] Sakai T, Jonas J J (1984) Overview n.35 Dynamic recrystallization: mechanical and microstructural considerations. *Acta Metal* 32(2): 189-209.  
[https://doi.org/10.1016/0001-6160\(84\)90049-X](https://doi.org/10.1016/0001-6160(84)90049-X).
- [20] Jonas J J (1994) Dynamic recrystallization - scientific curiosity or industrial tool? *Mater Sci Eng A* 184(2): 155–165.  
[https://doi.org/10.1016/0921-5093\(94\)91028-6](https://doi.org/10.1016/0921-5093(94)91028-6).
- [21] Hallberg H, Wallin M, Ristinmaa M (2010) Modeling of continuous dynamic recrystallization in commercial-purity aluminium. *Mater Sci Eng A* 527(4-5): 1126-1134.  
<https://doi.org/10.1016/j.msea.2009.09.043>.

- [22] Sakai T, Miura H, Yang X (2009) Ultrafine grain formation in face centered cubic metals during severe plastic deformation. *Mater Sci Eng A* 499(1-2): 2-6. <https://doi.org/10.1016/j.msea.2007.11.098>.
- [23] Yamagata H, Ohuchida Y, Saito N, Otsuka M (2001) Nucleation of new grains during discontinuous dynamic recrystallization of 99.998 mass% Aluminum at 453K. *Scr Mater* 45(9): 1055-1061. [https://doi.org/10.1016/S1359-6462\(01\)01139-3](https://doi.org/10.1016/S1359-6462(01)01139-3).
- [24] Iwahashi Y, Wang J, Horita Z, Nemoto M, Langdon T G (1996) Principle of equal-channel angular peessing for the processing of ultra-fine grained materials. *Scr Mater* 35(2): 143-146. [https://doi.org/10.1016/1359-6462\(96\)00107-8](https://doi.org/10.1016/1359-6462(96)00107-8).

# Figures

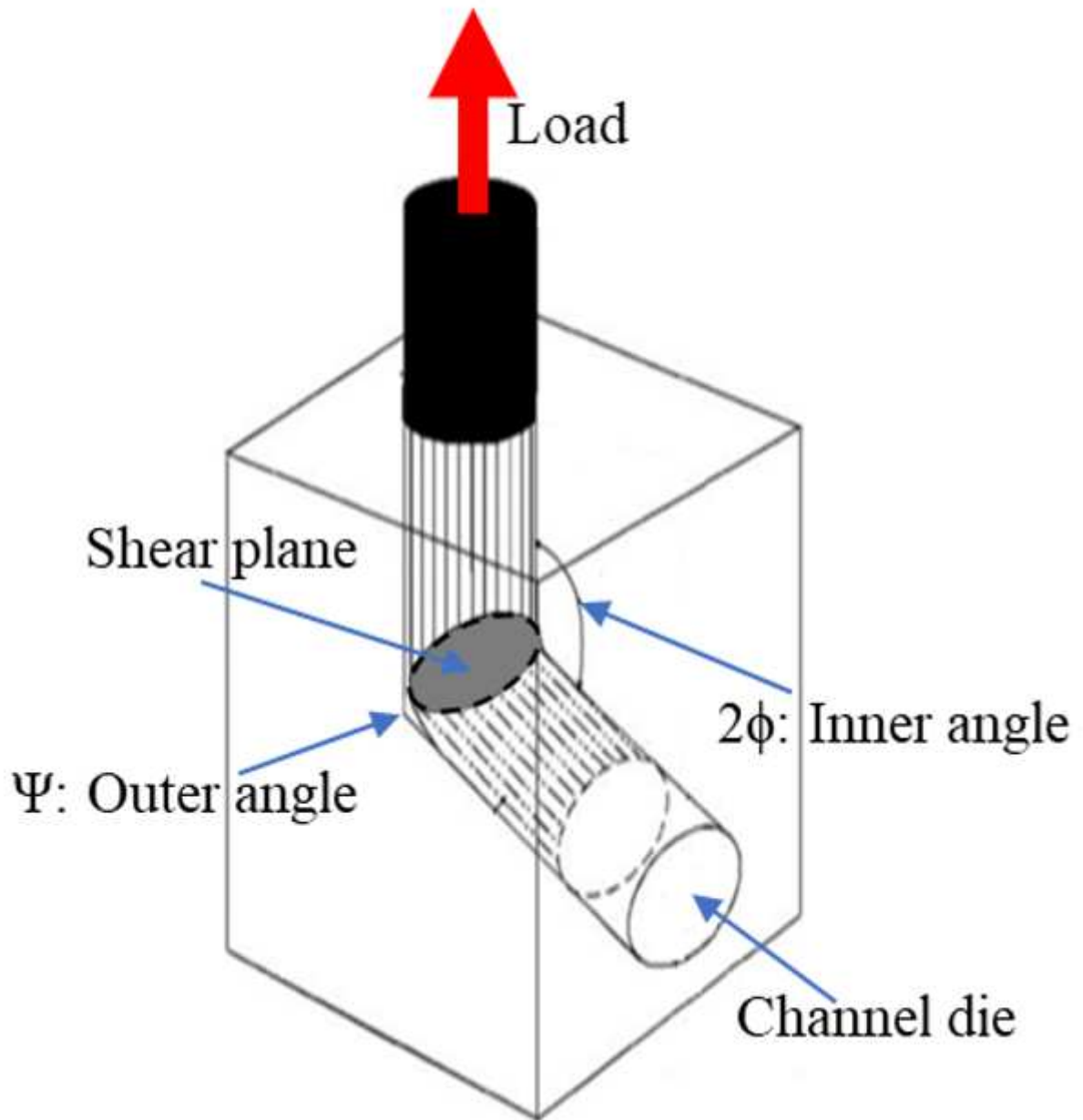


Figure 1

Schematic illustration of the ECAD process

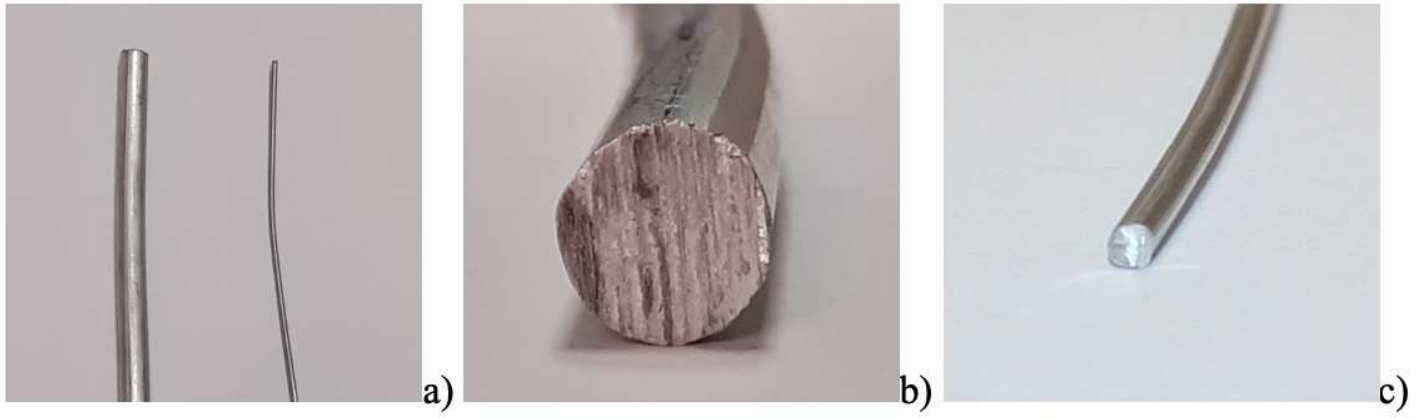


Figure 2

a) Analysed samples, b) Initial aluminium rod  $\Phi=9.50\text{mm}$ , c) Cold-drawn wire  $\Phi=2.00\text{mm}$

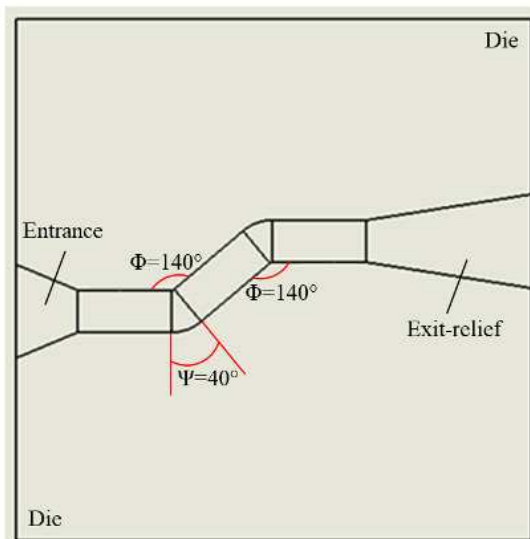


Figure 3

a-b) Geometry of the ECAD die, c-d) Experimental set-up

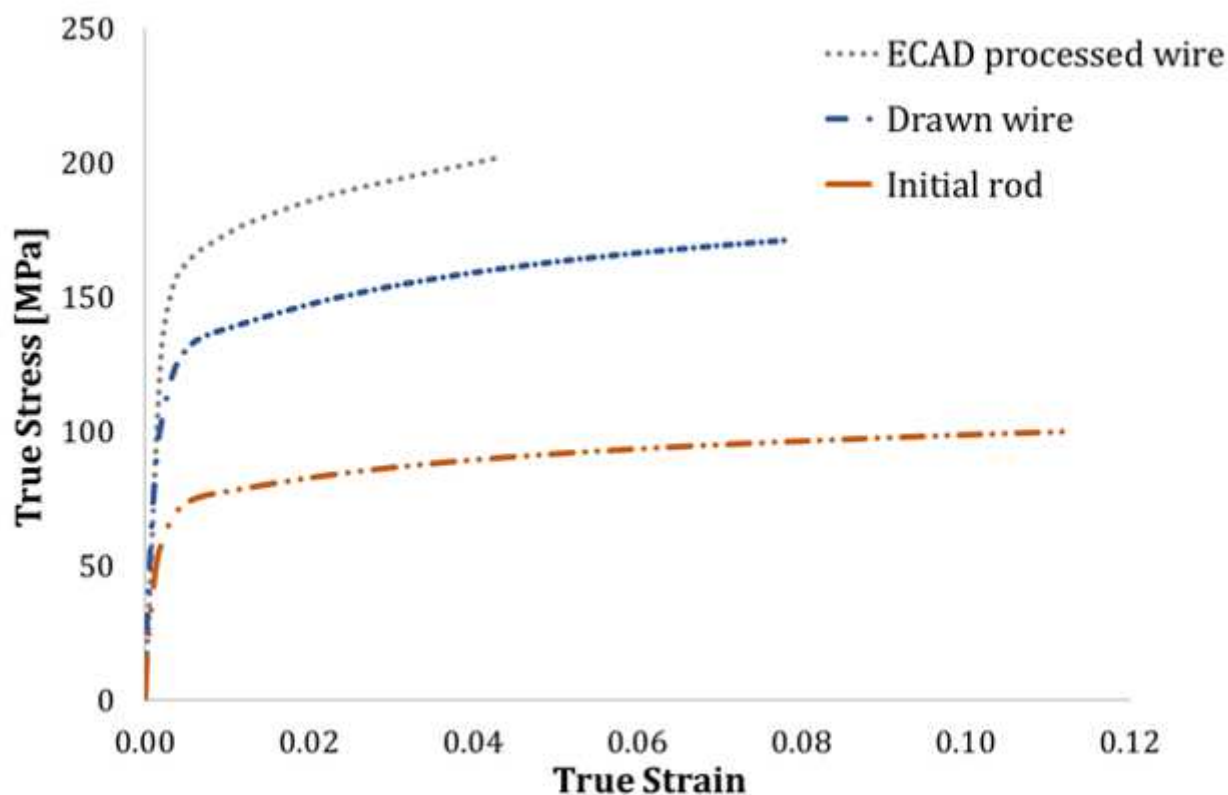


Figure 4

True stress-strain curve

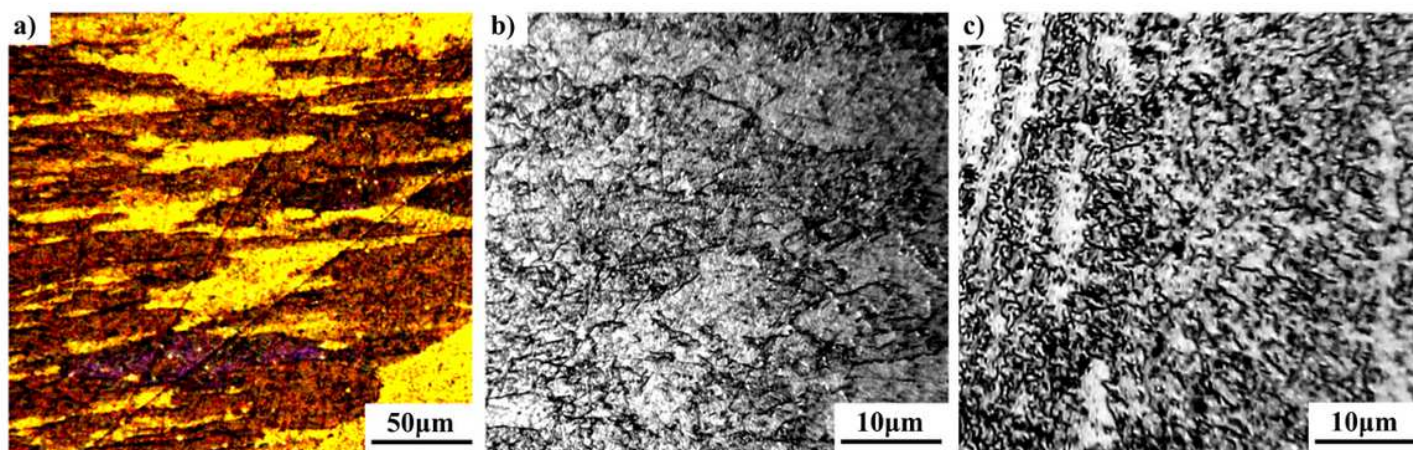
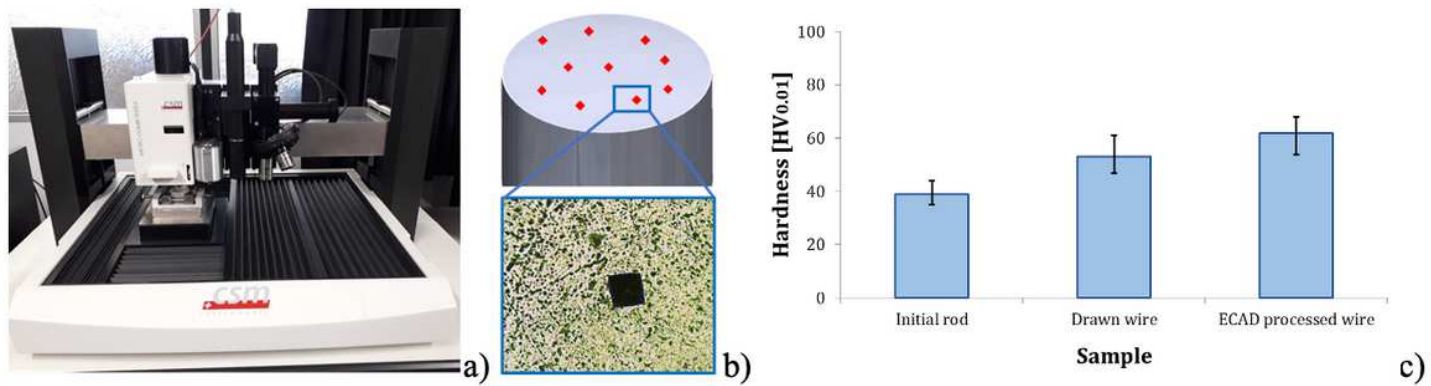


Figure 5

Transverse section microstructure a) initial aluminium rod (polarised light), b) cold-drawn wire (bright field) and c) ECAD processed wire (bright field)



**Figure 6**

Transverse section hardness a) micro-nano indenter, b) transverse section indentation analysis and c) measurements

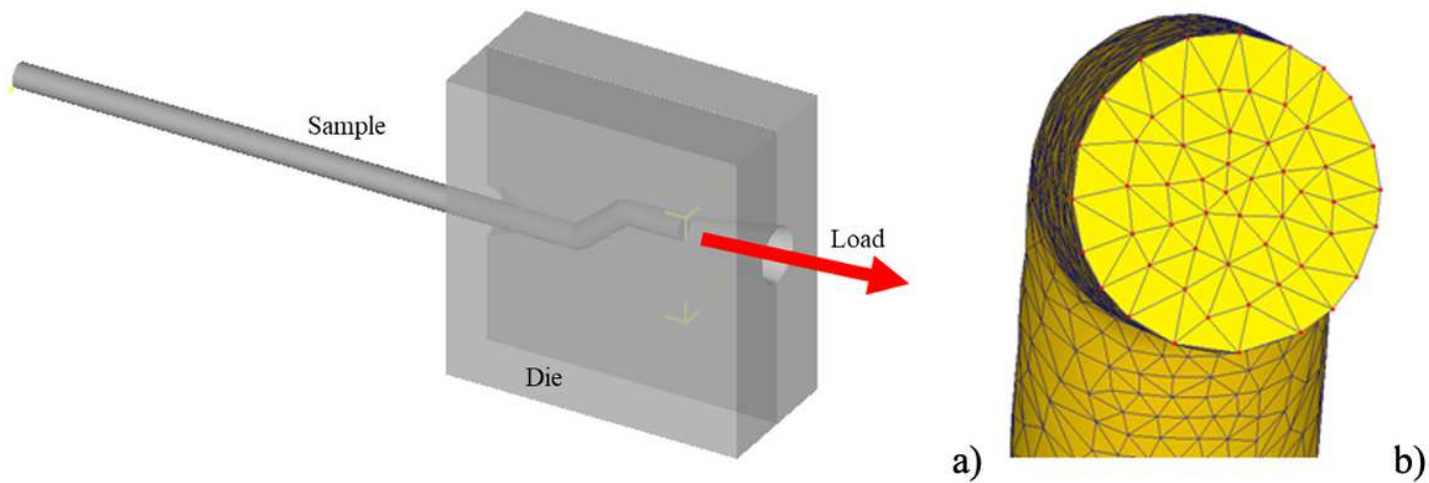


**Figure 7**

a) FE model and b) wires discretization

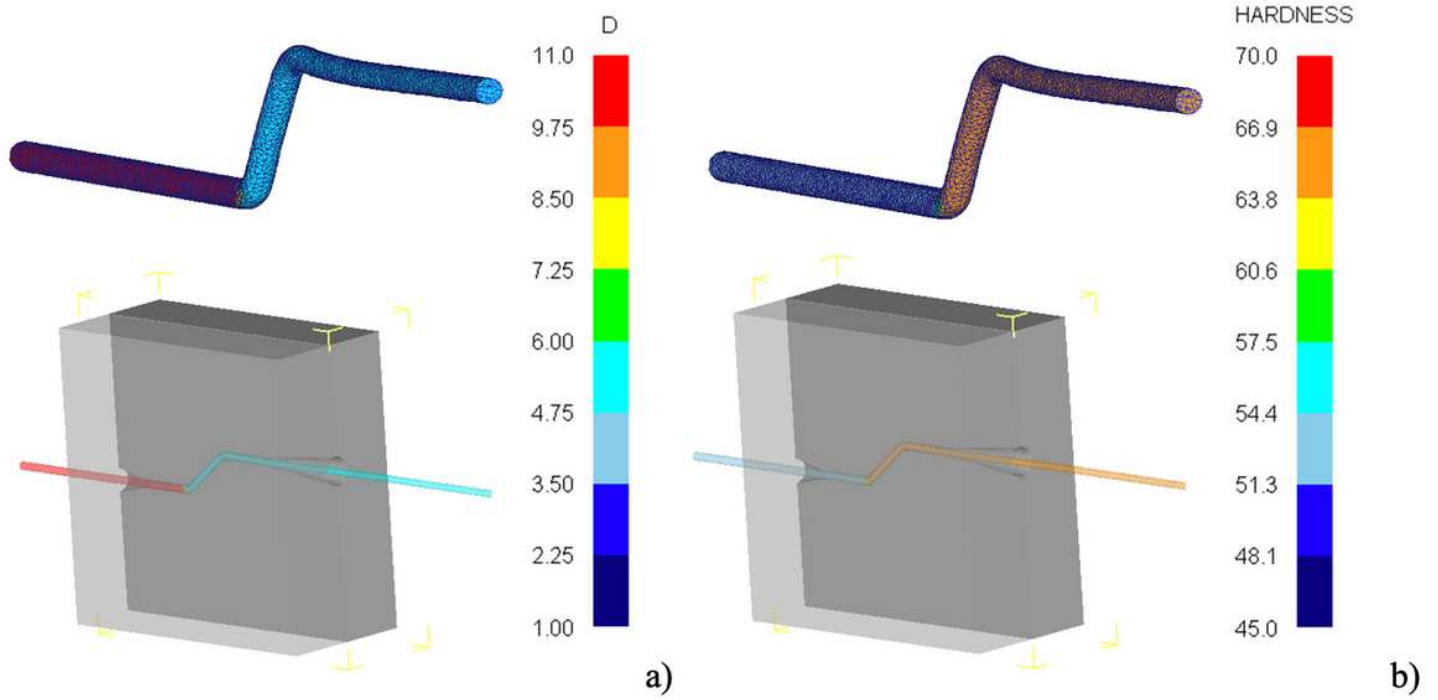


**Figure 8**

Numerical prediction of a) grain size ( $\mu\text{m}$ ) and b) hardness (HV0.01).

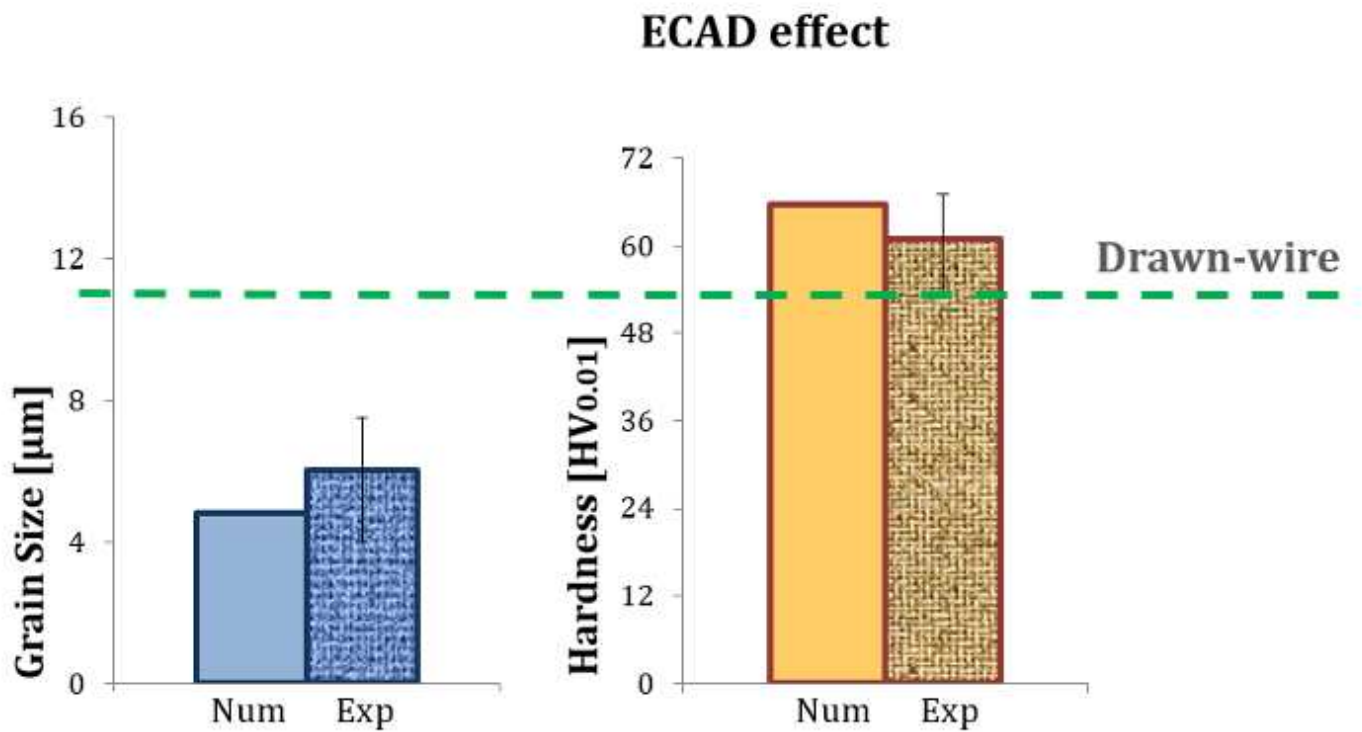


**Figure 9**

Comparison between measured and predicted grain size and hardness variation

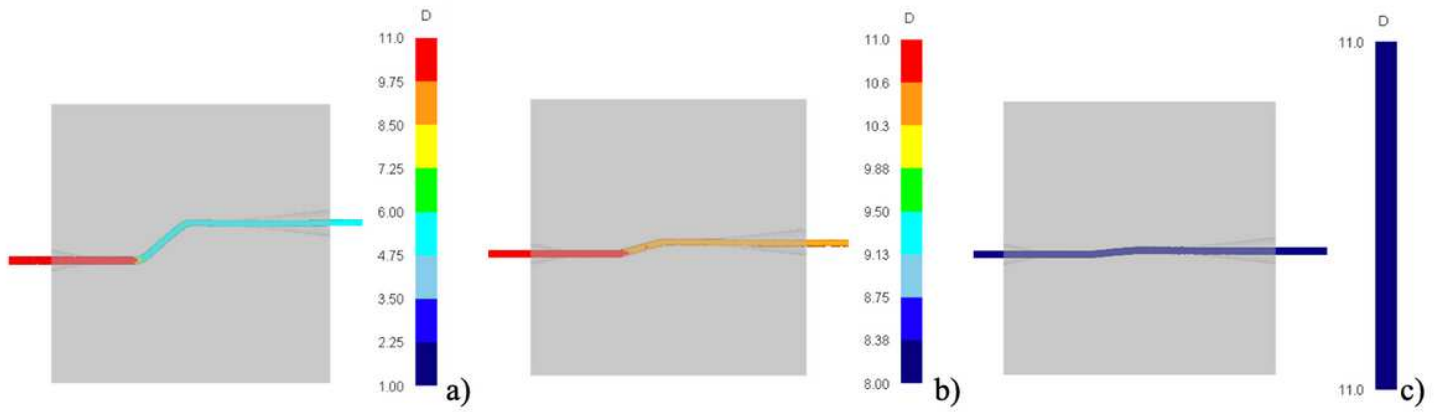


**Figure 10**

Grain size predictive numerical analysis: a)  $\Phi=140^\circ$ , b)  $\Phi=165^\circ$ , c)  $\Phi=175^\circ$

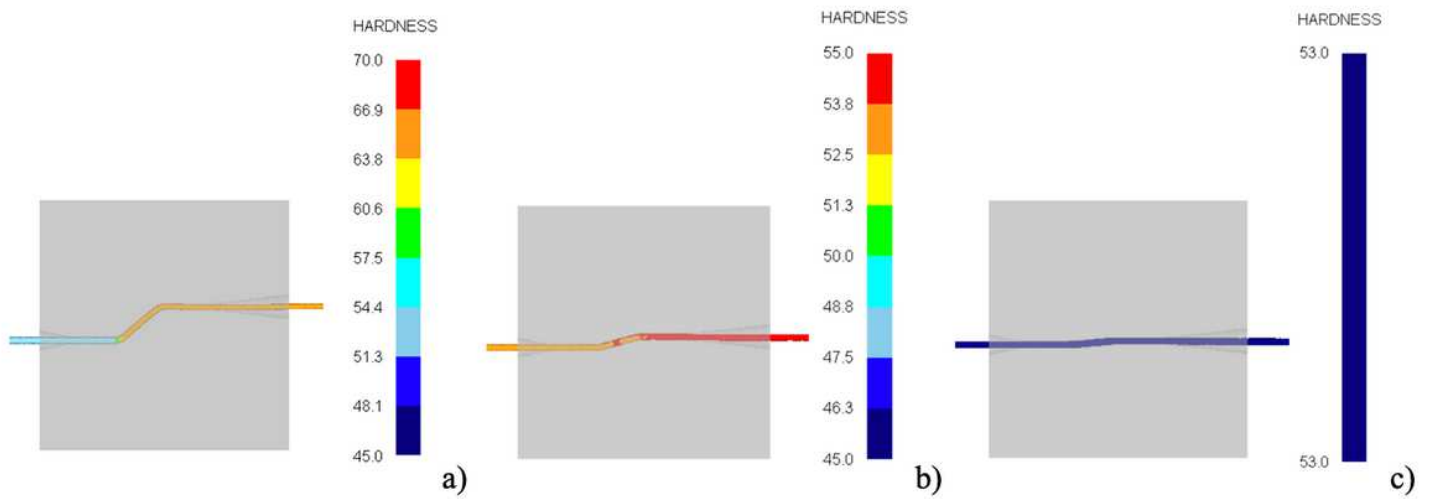


**Figure 11**

Hardness predictive numerical analysis: a)  $\Phi=140^\circ$ , b)  $\Phi=165^\circ$ , c)  $\Phi=175^\circ$